# Communications Employing 1-Bit Quantization and Oversampling at the Receiver: Faster-than-Nyquist Signaling and Sequence Design

Lukas Landau, Meik Dörpinghaus, and Gerhard Fettweis
Vodafone Chair Mobile Communications Systems
Technische Universität Dresden, 01062 Dresden, Germany
Email: {lukas.landau, meik.doerpinghaus, fettweis}@tu-dresden.de

***Abstract*—From circuit perspective, the resolution in time domain might be less difficult to achieve as compared to resolution in amplitude domain. Especially when considering Multigigabit communication the resolution in amplitude has remarkable power consumption. In this investigation some practical communication designs are proposed which exploit the utilization of 1-bit quantization and oversampling at the receiver. The proposed approach is the employment of faster-than-Nyquist QPSK signals in combination with an appropriate sequence design. Two sequence design strategies are proposed, namely the utilization of run-length limited sequences and the utilization of an optimized Markov source via an expectation based Blahut-Arimoto algorithm. Numerical results on the achievable data rate are computed based on an auxiliary channel lower bound which becomes tight in the high SNR regime. The results on the proposed methods and especially the run-length limited sequence based approach show superior performance in terms of achievable rate and spectral efficiency as compared to conventional signaling with independent and uniformly distributed symbols. Furthermore, the performance is close to and even above as compared to an analytical result on the achievable rate when sampling the sign of a bandlimited process given by Shamai.**

## I. Introduction

Multigigabit per second communication requires a corresponding analog-to-digital converter (ADC). Especially for wireless short range scenarios, such as given for communication between computer boards [1], an ADC with a sampling rate of multiple Gigasamples per second has remarkable impact on the total power consumption of the link. A popular method to obtain improved energy-efficiency of integrated circuits is to choose the supply voltage as small as possible. Nowadays a lot of circuits can be found which are based on a supply voltage that is smaller or equal to 1V. As a consequence the headroom for sophisticated processing in the amplitude domain is rather constrained [2]. On the other hand clock cycles become shorter which allows for higher sampling rates. In addition, the effective sampling rate can be further increased by considering multi-core circuits which can be utilized in a time interleaved fashion. All these circumstances indicate that achieving resolution in time domain is less challenging as compared to resolution in amplitude domain. In this regard, we investigate communications for systems where the receiver is equipped with a quantizer with 1-bit resolution. In order to compensate for the loss in terms of achievable rate the sampling rate might be chosen larger as compared to conventional designs which rely on fine grained quantization in amplitude domain. This special setup has been studied in [3]. One of the results is that the rate of

$$I = \log_2 \left(M_{\text{oversampling}} + 1\right) \text{[bits per Nyquist interval]}, \quad (1)$$

can be achieved when considering a real valued process which is sampled $M_{\text{oversampling}}$ times faster than the Nyquist rate w.r.t. the input bandwidth. However, this study does not consider noise and the waveform construction might require additional effort. The behavior in the low signal-to-noise ratio (SNR) regime is investigated in [4]. In [5] a practical approach has been studied, where we propose appropriate 4-ASK sequence designs which allow for reconstruction with 3fold oversampling and 1-bit quantization. Further, we have demonstrated in [6] that faster-than-Nyquist signaling [7] in combination with root raised cosine pulse shaping and independent and uniformly distributed (i.u.d.) input symbols is a suitable option for sampling with 1-bit quantization. A related topic has been addressed in [8], where the authors propose advanced deterministic dithering, which allows for waveform reconstruction considering a 1-bit quantizer. More recently, in [9] MIMO and SIMO systems with 1-bit quantization and sampling at Nyquist rate have been investigated.

In this paper, the approach of faster-than-Nyquist signaling with binary data (BPSK resp. QPSK) will be combined with sequence design. Different sequence design strategies will be proposed as an alternative to conventional i.u.d. symbols:

- run-length limited (rll) sequences,
- optimized sequences using an expectation based Blahut-Arimoto (BA) algorithm.

Finally our numerical evaluations show, that the rate in (1) can be attained by the proposed signaling schemes. Unlike the process construction in [3], the proposed methods are based on common signal processing building blocks.

We use the notation $x_{k-L}^{k} = [x_{k-L}, ..., x_k]^T$ and $x^n = [x_1, ..., x_n]^T$. Stacked vectors are denoted as $\boldsymbol{y}_{k-N}^{k} = [\boldsymbol{y}_{k-N}^T, ..., \boldsymbol{y}_k^T]^T$ and $\boldsymbol{y}^n = [\boldsymbol{y}_1^T, ..., \boldsymbol{y}_n^T]^T$. Probabilities and probability density functions are denoted by $P(\cdot)$ resp. $p(\cdot)$.

This work has been supported by the German Research Foundation in the framework of the Collaborative Research Center 912 "Highly Adaptive Energy-Efficient Computing".

978-1-4673-6555-0/15/$31.00 ©2015 IEEE

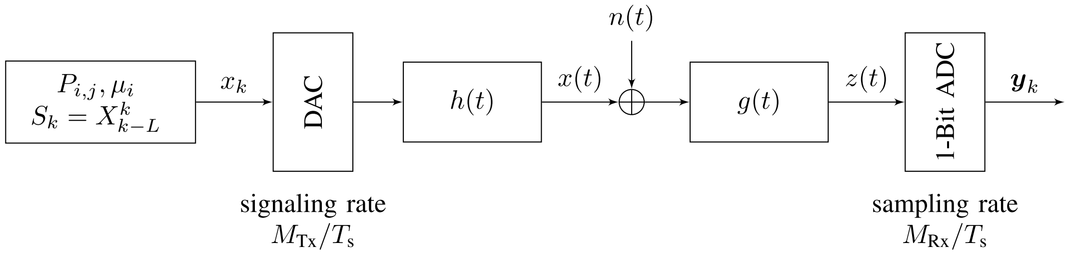


Fig. 1: System model, 1-bit quantization at the receiver

## II. System Model

The input symbols are QPSK symbols such that $x_k \in \left\{\frac{1+j}{\sqrt{2}}, \frac{1-j}{\sqrt{2}}, \frac{-1+j}{\sqrt{2}}, \frac{-1-j}{\sqrt{2}}\right\}$. Independent of signaling and sampling rate it is considered that the transmit filter is given by a raised and truncated cosine function

$$h\left(t\right) = \begin{cases} \sqrt{\frac{2}{3T_{\text{s}}}} \left(1 - \cos\left(2\pi \frac{1}{2T_{\text{s}}} t\right)\right), & 0 \leq t < 2T_{\text{s}} \\ 0, & \text{else}, \end{cases} \tag{2}$$

where $T_{\text{s}}$ is the reference time interval that relates to the signal bandwidth depending on the input distribution. The receive filter is an integrator

$$g\left(t\right) = \begin{cases} \sqrt{\frac{1}{T_{\text{s}}}}, & 0 \leq t < T_{\text{s}} \\ 0, & \text{else}, \end{cases} \tag{3}$$

which is a typical characteristic of a sampling circuit. Assuming a time-interleaved implementation of the sampling circuit, an increase of sampling rate will change the number of sampling cores, however the receive filter characteristic of the sampling device will remain the same. The waveform, which will be used to describe the received signals, is given by the convolution of both filters $v(t) = g(t) * h(t)$. In what follows, the discrete notations $\boldsymbol{v}_{\text{r}}, \boldsymbol{g}_{\text{r}}$ of $v(t), g(t)$ are used. The elements of $\boldsymbol{v}_{\text{r}}, \boldsymbol{g}_{\text{r}}$ are given by sampling time reversed $v(t)$ and $g(t)$ at rate $\frac{M_{\text{Rx}}}{T_{\text{s}}}$. The dimensions of the vectors $\boldsymbol{v}_{\text{r}}$ and $\boldsymbol{g}_{\text{r}}$ are given by $(L+1)M \times 1$ and $\xi M \times 1$. Further, perfect timing sync is assumed, such that the sampling instants in time include the peak-value of $v(t)$. The relation between signaling rate $\frac{M_{\text{Tx}}}{T_{\text{s}}}$ and sampling rate is given by $MM_{\text{Tx}} = M_{\text{Rx}}$. The generic notation for the received signal vector $\boldsymbol{z}_k$ and quantized signal vector $\boldsymbol{y}_k$ of length $M$ according to Fig. 1 is denoted as

$$\boldsymbol{y}_k = Q_1\left(\boldsymbol{z}_k\right) = Q_1\left(\boldsymbol{V}\boldsymbol{U}x_{k-L}^k + \boldsymbol{G}\boldsymbol{n}_{k-\xi}^k\right), \tag{4}$$

where $Q_1$ is the 1-bit quantizer having its threshold at 0, $x_{k-L}^k$ is a vector of $L+1$ consecutive transmit symbols, and $\boldsymbol{n}_{k-\xi}^k$ is a vector of $M\left(\xi+1\right)$ noise samples. The waveform resp. receive filter matrices are denoted as

$$\boldsymbol{V} = \begin{pmatrix} [\ \boldsymbol{v}_{\text{r}}^T\ ] & 0 \cdots & 0 \\ 0 & [\ \boldsymbol{v}_{\text{r}}^T\ ] & 0 \cdots 0 \\ & \ddots\ \ddots\ \ddots & \\ 0 \cdots & 0 & [\ \boldsymbol{v}_{\text{r}}^T\ ] \end{pmatrix}, \quad \boldsymbol{G} = \begin{pmatrix} [\ \boldsymbol{g}_{\text{r}}^T\ ] & 0 \cdots & 0 & 0 \\ 0 & [\ \boldsymbol{g}_{\text{r}}^T\ ] & 0 \cdots 0 & 0 \\ & \ddots\ \ddots\ \ddots & & \\ 0 \cdots & 0 & [\ \boldsymbol{g}_{\text{r}}^T\ ] & 0 \end{pmatrix}, \tag{5}$$

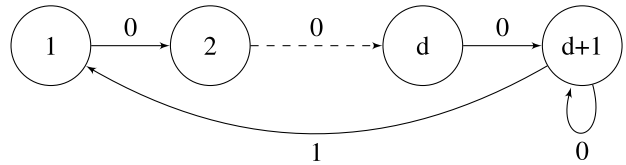


Fig. 2: State machine for a d-constrained sequence

where $\boldsymbol{V}$ has the dimension $M \times M(L+2)-1$ and $\boldsymbol{G}$ has the dimension $M \times M(\xi+1)$. The upsampling matrix with dimension $M(L+2)-1 \times L+1$ is described by

$$U_{i,j} = \begin{cases} 1 & \text{for } i = j \cdot M \\ 0 & \text{else}, \end{cases} \tag{6}$$

where $i$ indicates the row and $j$ indicates the column. In what follows, the special case, where signaling and sampling rate are equal, i.e., $M = 1$, is considered. When considering a signaling/sampling rate with $M_{\text{Rx}} = M_{\text{Tx}} > 1$ each sample $\boldsymbol{y}_k$ also depends on previous input symbols $x^{k-1}$. In this case the corresponding channel can be called channel with memory. Indeed, an appropriate input sequence resp. signal source for a channel with memory is itself characterized by memory [10]. Hence, a Markov source is considered with the property $P\left(x_k|x^{k-1}\right) = P\left(x_k|x_{k-N}^{k-1}\right) = P\left(s_k|s_{k-1}\right)$. In this regard the state of the Markov source is given by $S_k = X_{k-N+1}^k$. Its stationary distribution is $\mu_i = P\left(S_k = i\right)$ and the transition probabilities are $P_{i,j} = P\left(S_k = j|S_{k-1} = i\right)$.

## III. Run-Length Limited Sequences

Run-length limited sequences are known from magnetic recording. Some of the main results on run-length limited sequences are summarized in [11]. The run-length limited sequence can be obtained from a so called $(d, k)$ sequence, where $d$ and $k$ are parameters which constrain the sequences. A $(d, k)$ sequence is a binary sequence where a one is followed by at least $d$ and at most $k$ zeros. The $k$ property is introduced for practical purpose such as clock recovery what we will neglect in this work which means that $k = \infty$. A corresponding state machine for a $d$ constrained sequence is illustrated in Fig. 2. The $(d, k)$ sequence can be transferred to a run-length limited sequence by realizing a sign-flip whenever a one occurs. An example is given as follows

$$\begin{aligned}(d,\,k)\ \text{seq.} &= [...1,0,0,\quad 1,\quad 0,\quad 1,0,0,\quad 1,\quad 0...]\\ \text{rll seq.} &= [...1,1,1,\quad -1,\quad -1,\quad 1,1,1,\quad -1,\quad -1...]\quad .\end{aligned}$$

According to [12] the maximum entropy rate of such a sequence, which corresponds to the maximum transmission rate, can be computed with

$$H_{\text{max}} = \lim_{n\to\infty} \frac{1}{n} \log_2 \sum_{i,j} [\mathbf{D}^n]_{i,j} = \log_2(\lambda), \tag{7}$$

where $\mathbf{D}$ is the adjacency matrix, which describes the directional connections of the state machine in Fig. 2 generating $d$ constrained sequences and $\lambda$ is the largest eigenvalue of the adjacency matrix. The adjacency matrix can be expressed by

$$\mathbf{D}_{d=1} = \begin{bmatrix} 0 & 1 \\ 1 & 1 \end{bmatrix}\ ,\quad \mathbf{D}_{d=2} = \begin{bmatrix} 0 & 1 & 0 \\ 0 & 0 & 1 \\ 1 & 0 & 1 \end{bmatrix}, \tag{8}$$

where the rows correspond to the current states and the columns correspond to the following state. Furthermore the transition probabilities for the max entropic source can be found with

$$P_{i,j} = \frac{b_j}{b_i} \cdot \frac{D_{i,j}}{\lambda}, \tag{9}$$

where $b_i$ and $b_j$ are entries of the right-sided eigenvector corresponding to the eigenvalue $\lambda$. With increasing $d$ the redundancy in the sequence increases such that the entropy rate is decreasing as listed in Table I. However, such a sequence design is able to cope with a channel with memory. As a consequence this allows for faster signaling rates and finally this is beneficial in terms of the achievable rate.

TABLE I: Maximum entropy of d-constrained sources

| run-length constraint | $d=1$ | $d=2$ | $d=3$ | $d=4$ |
|---|---|---|---|---|
| max entropy rate [bit/symbol] | 0.6942 | 0.5515 | 0.4650 | 0.4057 |

## IV. Markov Source Optimized by an Expectation Based Blahut-Arimoto Algorithm

In this section an algorithm is proposed which optimizes a Markov source w.r.t. a lower bound on $\lim_{n\to\infty} \frac{1}{n} I(X^n;\boldsymbol{Y}^n)$. Following the steps in [13] it can be shown that the achievable rate can be lower bounded by utilizing the Shannon-McMillan-Breiman theorem and an auxiliary channel model as follows

$$\begin{aligned}\lim_{n\to\infty} \frac{1}{n} I(X^n;\boldsymbol{Y}^n) &\geq \frac{1}{n}(-\log P(x^n) + \log W(x^n|\boldsymbol{y}^n))\\ &= \frac{1}{n}(-\log P(s^n) + \log W(s^n|\boldsymbol{y}^n)),\end{aligned} \tag{10}$$

for large $n$ on the right hand side where $W(\cdot)$ is the channel law of the auxiliary channel, $x^n$ is a realization of a very long input sequence and $\boldsymbol{y}^n$ is the corresponding output sequence. The only requirement on $W(\cdot)$ is that it is larger than 0 whenever $P(\cdot)$ is larger than 0. Similar to what is proposed in [14], (10) can be reformulated, such that it is possible to factor out $P_{i,j}$ which describe the Markov source. Finally, it can be written in the format which is known from the expectation based Blahut-Arimoto algorithm [14]

$$\lim_{n\to\infty} \frac{1}{n} I\left(X^n;\boldsymbol{Y}^n\right) \geq \sum_{i,j} \mu_i P_{i,j} \left(\log_2\left(\frac{1}{P_{i,j}}\right) + \hat{T}_{i,j}\right). \tag{11}$$

The utilization of the auxiliary channel requires an alternative computation of the elements $\hat{T}_{i,j}$ as compared to [14]. The elements can be computed by

$$\hat{T}_{i,j} = \left\{ \frac{\left[\sum_{k\left|\substack{s_{k-1}\,=\,i\\ s_k\,=\,j}\right.} \log_2 W\left(s_k, s_{k-1}|\boldsymbol{y}^n\right)\right]}{\left[\sum_{k\left|\substack{s_{k-1}\,=\,i\\ s_k\,=\,j}\right.} 1\right]} - \frac{\left[\sum_{k|s_k\,=\,i} \log_2 W\left(s_k|\boldsymbol{y}^n\right)\right]}{\left[\sum_{k|s_k\,=\,i} 1\right]} \right\}, \tag{12}$$

where $W\left(s_k, s_{k-1}|\boldsymbol{y}^n\right)$ resp. $W\left(s_{k-1}|\boldsymbol{y}^n\right)$ are computed with a BCJR algorithm [15]. In order to successively increase the achievable rate per channel use the optimized Markov source transition probabilities can be computed by

$$P_{i,j} = \frac{b_j}{b_i} \frac{A_{i,j}}{W_{\text{max}}}, \tag{13}$$

where $A_{i,j}$ are the entries of a noisy adjacency matrix $\boldsymbol{A}$ computed by

$$A_{i,j} = 2^{\hat{T}_{i,j}}. \tag{14}$$

Further $W_{\text{max}}$ is the largest real eigenvalue of $\boldsymbol{A}$ and $\boldsymbol{b}$ is the corresponding eigenvector. Based on the updated transition probabilities $P_{i,j}$ a new sequence $x^n$ can be generated for repeating the computation. Especially for the high SNR regime the iterative process converges after a few iterations. As mentioned before, based on this approach we optimize the source in order to benefit in terms of achievable rate.

## V. Computation of the Achievable Rate

For a numerical evaluation, a lower bound on the achievable rate is computed, following the approach in [13] by using the method derived in [16]. The lower bound based on the auxiliary channel is given by

$$\lim_{n\to\infty} \frac{1}{n} I(X^n;\boldsymbol{Y}^n) \geq \frac{1}{n}(-\log_2 W(\boldsymbol{y}^n) + \log_2 W(\boldsymbol{y}^n|s^n)), \tag{15}$$

where the auxiliary channel $W(\cdot)$ is based on the approximation $P(\boldsymbol{y}_k|\boldsymbol{y}^{k-1}, x^k) \approx P(\boldsymbol{y}_k|x_{k-L}^k)$. An even tighter bound in the low SNR regime can be computed by following strategies presented in [16], where previous channel realizations, e.g., $\boldsymbol{y}_{k-1}$, are considered in the auxiliary channel model. Moreover, (15) corresponds to less computational effort as compared to (10), as only the forward recursion of the BCJR algorithm needs to be carried out. The quantities can be computed with

$$W(\boldsymbol{y}^k) = \sum_{s_k} W(\boldsymbol{y}^k, s_k), \tag{16}$$

$$W(\boldsymbol{y}^k, s_k) = \sum_{s_{k-1}} P(\boldsymbol{y}_k|s_k, s_{k-1}) P(s_k|s_{k-1}) W(\boldsymbol{y}^{k-1}, s_{k-1})$$

resp.

$$W(\boldsymbol{y}^k|s^n) = P\left(\boldsymbol{y}_k|s_{k-1}, s_k\right) W(\boldsymbol{y}^{k-1}|s^n). \tag{17}$$

Its transition probability is obtained by integration over the pdf of the unquantized signal

$$P(\boldsymbol{y}_k|s_k, s_{k-1}) = \int\limits_{\boldsymbol{z}_k \in \mathbb{Y}_k} p(\boldsymbol{z}_k|s_k, s_{k-1}) d\boldsymbol{z}_k, \tag{18}$$

where $\mathbb{Y}_k$ denotes the quantization region corresponding to the output $\boldsymbol{y}_k$. In general the pdf is a multivariate Gaussian distribution

$$\begin{aligned} p\left(\boldsymbol{z}_k|s_{k-1}^k\right) =& p\left(\boldsymbol{z}_k|x_{k-L}^k\right) \\ =& \frac{1}{\pi^M |\boldsymbol{R}|} \mathrm{e}^{\left(-(\boldsymbol{z}_k-\boldsymbol{\mu}_x)^H \boldsymbol{R}^{-1} (\boldsymbol{z}_k-\boldsymbol{\mu}_x)\right)}, \end{aligned} \tag{19}$$

with the mean vector $\boldsymbol{\mu}_x = \boldsymbol{V}\boldsymbol{U}x_{k-L}^k$ and the covariance matrix $\boldsymbol{R} = \mathrm{E}\{\boldsymbol{G}\boldsymbol{n}_{k-\xi}^k (\boldsymbol{n}_{k-\xi}^k)^H \boldsymbol{G}^H\}$.

## VI. Spectrum and Spectral Efficiency

The power spectral density $S(f)$ of the transmit signal depends on the transmit filter (2) and on the autocorrelation function of the input sequence $x^n$ which can be computed by

$$\begin{aligned} c_k &= \mathrm{E}\left\{x_l x_{l-k}^*\right\} = \boldsymbol{x}^H \boldsymbol{P}^k \mathrm{diag}\left\{\boldsymbol{\mu}\right\} \boldsymbol{x} && k \geq 0 \\ c_k &= c_{-k}^* && k < 0, \end{aligned} \tag{20}$$

where $\boldsymbol{P}$ contains the transition probabilities $P_{i,j}$, $\boldsymbol{\mu}$ contains the stationary distribution $\mu_i$, and $\boldsymbol{x}$ represents $x_k$ according to the set of states of $S_k$ of the Markov source model. Each entry of the vector $\boldsymbol{x}$ corresponds to one possible state of $S_k$. Indeed, the spectrum of the transmit signal is not strictly bandlimited. For computing the spectral efficiency instead of the absolute bandwidth, the $90\%$ power containment bandwidth [17] has been considered. In this regard, $5\%$ out of band radiation is allowed at the lower frequencies resp. higher frequencies

$$\int_{-\infty}^{B_{90\%,\uparrow}} S(f) df = \int_{B_{90\%,\downarrow}}^{\infty} S(f) df = 0.95 \int_{-\infty}^{\infty} S(f) df. \tag{21}$$

Finally the two sided bandwidth is given by $B_{90\%} = B_{90\%,\uparrow} - B_{90\%,\downarrow}$. Based on the achievable rate and the bandwidth a spectral efficiency in bits per second per Hertz can be defined as

$$\text{spectral eff.} = \frac{I_{\text{bpcu}} M_{\text{Tx}}}{T_{\text{s}} B_{90\%}}, \tag{22}$$

where $I_{\text{bpcu}}$ is the mutual information w.r.t. a symbol $x_k$.

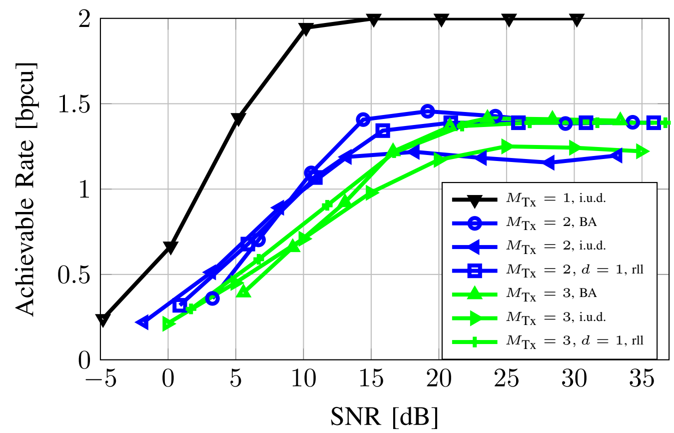


Fig. 3: Achievable rate versus SNR in bits per channel use for for different sequence designs

## VII. Numerical Results

For numerical computations sequences of length $n = 10^6$ are considered. The SNR is defined by

$$SNR = \frac{\lim_{T\to\infty} \frac{1}{T} \int_T |x(t)|^2 dt}{N_0 \; B_{90\%}}. \tag{23}$$

For the evaluation complex modulation is considered, such that the rate corresponding to runlength-limited sequences is doubled as compared to Table I. Fig. 3 illustrates the achievable rate in terms of bits per channel use, where a channel use corresponds to an input symbol $x_k$. While the achievable rate considering i.u.d. input symbols is significantly below the input entropy rate of 2 bits per channel use for $M_{\text{Tx}} > 1$, the achievable rate of the $d$-constrained run-length limited sequence approaches the input entropy rate of $2 \times 0.6942$ bits per channel use in both cases. In some cases slightly better performance in terms of bits per channel use can be obtained by the expectation based Blahut-Arimoto algorithm. However, in Fig. 3 bandwidth and signaling rate are not taken into account. In this regard, Fig. 4 illustrates the spectral efficiency as a reasonable comparison, where run-length limited sequences significantly outperform the approach based on the expectation based Blahut-Arimoto algorithm and also the approach based on i.u.d. symbol sequences. In Fig. 5 the corresponding power spectral densities are plotted for run-length limited sequences and i.u.d. sequences. The power spectral densities of the sequences optimized by the expectation based Blahut-Arimoto algorithm, which depend on the SNR, are not shown. Finally, the results are compared with one of the expressions for the achievable rate given in [3], see (1), which itself is a lower bound on the capacity. In this regard, the effective oversampling factor is computed by

$$M_{\text{oversampling}} = T_{\text{sampling}} B_{90\%} = \frac{T_{\text{s}} B_{90\%}}{M_{\text{Rx}}} \tag{24}$$

The results are given in Table II and Fig. 6, which also show the influence of the signaling method on the bandwidth by the relation between $M_{\text{Tx}}$ and $M_{\text{oversampling}}$.

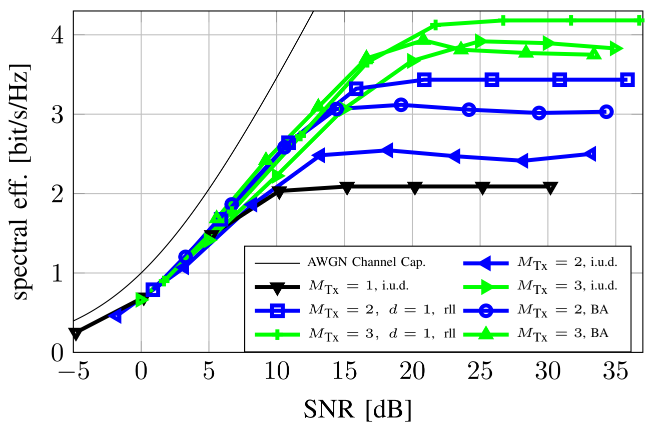


Fig. 4: Spectral efficiency versus SNR for different sequence designs

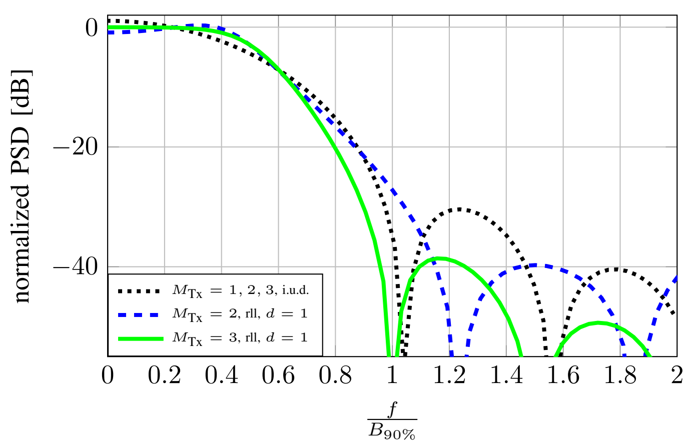


Fig. 5: Power spectral density

## VIII. Conclusions

In this investigation it is shown how to combine sequence design and faster-than-Nyquist signaling resp. sampling using QPSK signals for the reception with receivers equipped with a 1-bit quantizer. The numerical results strongly indicate, that the proposed utilization of run-length limited sequences is an appropriate choice in terms of spectral efficiency. The proposed method significantly outperforms the conventional approach based on i.u.d. symbols. The proposed method yields an achievable rate that is comparable or slightly above the analytical reference in [3]. In addition, an expectation based Blahut-Arimoto algorithm is proposed which optimizes the performance in terms of bits per channel use for an auxiliary channel model.

TABLE II: Comparison to [3] with effective oversampling factor and maximum spectral efficiency over the SNR

| | $M_{\mathrm{Tx}} = M_{\mathrm{Rx}}$ | $M_{\mathrm{oversampling}}$ | max spectral eff. [bit/s/Hz] | $2\log_2(M_{\mathrm{oversampling}}+1)$ [bit/s/Hz] |
|---|---|---|---|---|
| i.u.d. | 1 | 1.0448 | 2.0897 | 2.0639 |
| | 2 | 2.0897 | 2.5454 | 3.2548 |
| | 3 | 3.1346 | 3.9181 | 4.0954 |
| rll | 2 | 2.4734 | 3.4344 | 3.5927 |
| | 3 | 3.0117 | 4.1819 | 4.0084 |
| BA | 2 | 2.1422 | 3.1182 | 3.3036 |
| | 3 | 2.8764 | 3.9315 | 3.9094 |

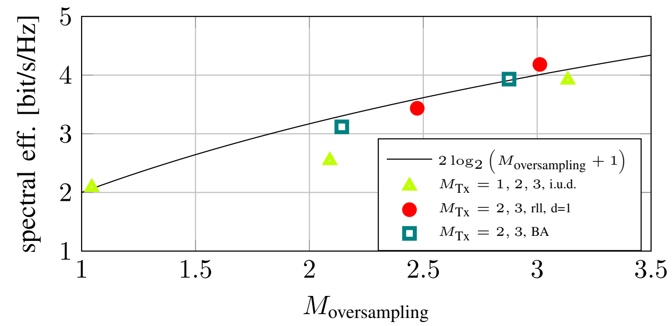


Fig. 6: Comparison with analytical result in [3], interpolated

## References


[1] G. P. Fettweis, N. ul Hassan, L. Landau, and E. Fischer, "Wireless interconnect for board and chip level," in *Proc. of the Conference on Design, Automation & Test in Europe*, 2013, (invited).

[2] R. B. Staszewski, "Digitally intensive wireless transceivers," *IEEE Design & Test of Computers*, vol. 29, no. 6, pp. 7–18, 2012.

[3] S. Shamai (Shitz), "Information rates by oversampling the sign of a bandlimited process," *IEEE Trans. Inf. Theory*, vol. 40, no. 4, pp. 1230–1236, 1994.

[4] T. Koch and A. Lapidoth, "Increased capacity per unit-cost by oversampling," in *Proc. of the IEEE Convention of Electrical and Electronics Engineers in Israel*, 2010.

[5] L. Landau and G. P. Fettweis, "On reconstructable ASK-sequences for receivers employing 1-bit quantization and oversampling," in *Proc. of the IEEE International Conference on Ultra-Wideband*, 2014.

[6] T. Hälsig, L. Landau, and G. P. Fettweis, "Information rates for faster-than-Nyquist signaling with 1-bit quantization and oversampling at the receiver," in *Proc. of the IEEE Vehicular Technology Conference (Spring)*, 2014.

[7] J. E. Mazo, "Faster-than-Nyquist signaling," *Bell System Technical Journal*, vol. 54, no. 1, pp. 1451–1462, 1975.

[8] Z. Cvetkovic, I. Daubechies, and J. Logan, B.F., "Single-bit oversampled a/d conversion with exponential accuracy in the bit rate," *IEEE Trans. Inf. Theory*, vol. 53, no. 11, pp. 3979–3989, Nov 2007.

[9] J. Mo and R. W. Heath, "High snr capacity of millimeter wave mimo systems with one-bit quantization," in *Proc. of Information Theory and Applications Workshop (ITA), 2014*, Feb 2014, pp. 1–5.

[10] J. Chen and P. H. Siegel, "Markov processes asymptotically achieve the capacity of finite-state intersymbol interference channels," *IEEE Trans. Inf. Theory*, vol. 54, no. 3, pp. 1295–1303, 2008.

[11] K. A. Schouhamer Immink, "Runlength-limited sequences," *Proc. of the IEEE*, vol. 78, no. 11, pp. 1745–1759, Nov 1990.

[12] C. E. Shannon, "A mathematical theory of communications," *Bell System Technical Journal*, vol. 27, pp. 379–423, Jul. 1948.

[13] D. M. Arnold, H.-A. Loeliger, P. O. Vontobel, A. Kavcic, and W. Zeng, "Simulation-based computation of information rates for channels with memory," *IEEE Trans. Inf. Theory*, vol. 52, no. 8, pp. 3498–3508, 2006.

[14] A. Kavcic, "On the capacity of Markov sources over noisy channels," in *Proc. IEEE Glob. Comm. Conf. (GLOBECOM)*, vol. 5, 2001, pp. 2997–3001 vol.5.

[15] L. Bahl, J. Cocke, F. Jelinek, and J. Raviv, "Optimal decoding of linear codes for minimizing symbol error rate (corresp.)," *IEEE Trans. Inf. Theory*, vol. 20, no. 2, pp. 284–287, Mar 1974.

[16] L. Landau and G. P. Fettweis, "Information rates employing 1-bit quantization and oversampling," in *Proc. of the IEEE Int. Workshop on Signal Processing Advances in Wireless Communications*, 2014.

[17] U. Madhow, *Fundamentals of Digital Communication*. Cambridge University Press, 2008, Cambridge Books Online. [Online]. Available: http://dx.doi.org/10.1017/CBO9780511807046